Available online at www.sciencedirect.com
ScienceDirect
Journal of Molecular Catalysis A: Chemical 280 (2008) 194–202
JOURNAL OF MOLECULAR CATALYSIS A: CHEMICAL
www.elsevier.com/locate/molcata

Calculation of the energy of adsorption of *n*-paraffins in nanoporous crystalline and ordered acid catalysts, and its relationship with the activation energy of the monomolecular catalytic cracking reaction

Rolando Roque-Malherbe *, F. Diaz-Castro

Institute of Physical Chemical Applied Research, School of Science, Turabo University, PO Box 3030, Gurabo, PR 00778-3030, USA

Received 27 September 2007; received in revised form 13 November 2007; accepted 14 November 2007
Available online 22 November 2007

Abstract

Applying the Horvath–Kawazoe approach for: the slit, cylindrical and spherical pore models for the description of the geometry of the channels and cavities of nanoporous materials, and the united-atom model to describe *n*-alkanes of, *m*, carbons; were calculated mathematical expressions to describe the enthalpy of adsorption of these alkanes in acid nanoporous materials, such as zeolites and mesoporous molecular sieves. After that, applying ideas developed by Haag, Gorte and others, and the transition state theory, the expressions for the enthalpy of adsorption were linked with the observed and intrinsic activation energies for the unimolecular catalytic cracking reaction. To evaluate the implicit mathematical expressions for the enthalpy of adsorption were used parameters which characterize methane and the adsorbent surface, and was carried out a detailed experimental analysis of the pore diameters of the tested materials. The obtained numerical equations were plotted and tested with reliable literature data, obtaining results which fairly well coincide with the reported experimental values.

Keywords: Monomolecular cracking; Activation energy; Adsorption enthalpy; Pore geometry

1. Introduction.

1.1. General introduction

Catalytic cracking is an industrial chemical operation for the conversion of vacuum distillates and residues into olefinic gas, high-octane gasoline and diesel oil [1–3]. This is accomplished by cracking a vaporized feed over a solid acid catalyst [1]. Zeolites, pillared clays, and mesoporous molecular sieves can be grouped as crystalline and ordered nanoporous materials. The acid forms of these materials have been applied in catalytic cracking or have been investigated to be applied in these reactions [2,3].

Even though, it is usually accepted that Brönsted acid centers are implicated in these reactions [2,3], efforts to associate the number of protons and their acid strength to a particular catalytic reaction have frequently led to incoherent results, particularly in the instance when are evaluated the catalytic properties of different structures [4]. That is, as was stated by Derouane: one should not be prompt to assign differences in reactivity for two different structures only to dissimilarities in acid strengths [5].

As noted by Haag the complexity in making evaluations may result from the fact that the concentration effect is not adequately treated [6]. Specifically, zeolites have diverse adsorption characteristics that will effect the local concentration of hydrocarbons within the cavities or channels. Then, this enhancement in reactant concentration, relative to the gas phase, may be viewed as a sorption effect or as a confinement effect [6,7]. Therefore, given that the effect of zeolite structure on the heat of adsorption can be noticeable, subsequently, the reaction rates can be markedly different for two zeolite structures, even if the acid sites are similar [8].

* Corresponding author. Tel.: +1 787 743 7979x4260; fax: +1 787 744 5427.
E-mail addresses: RRoque@suagm.edu, RRoquemalh@aol.com (R. Roque-Malherbe).

1381-1169/$ – see front matter © 2007 Elsevier B.V. All rights reserved.
doi:10.1016/j.molcata.2007.11.011

In the concrete case, of alkane cracking, dispersion forces between the alkane molecules and the siliceous walls of the zeolites and perhaps other nanoporous crystalline and ordered materials, are probably the most significant interactions for stabilizing adsorption in the cavities [8]. Because, the proton affinity of alkanes is low [8] and the electrostatic interactions between the alkane and the adsorbent are as well negligible.

The present paper aims to complement some ideas developed by Haag [6], Gorte [7,8] and others [4,9,10] employing the: slit [11], cylindrical [12] and spherical pore models [13] for the description of the channels and cavities of acid nanoporous crystalline materials, such as zeolites, and pillared clays (PILCs), and ordered nanoporous materials, such as, the mesoporous molecular sieves (MMS) [2,3]. With the developed model we will describe alkane adsorption in nanoporous crystalline and ordered acid catalysts in order to calculate three mathematical expressions, one for each pore geometry, to describe the adsorption enthalpy and its relation with the activation energy for the monomolecular cracking of *n*-paraffins. The developed methodology could be as well applied to other unimolecular reactions.

1.2. Unimolecular alkane catalytic cracking

It has been proposed that hydrocarbon cracking operates by means of two mechanisms, i.e., monomolecular and bimolecular [9,10]. In the monomolecular cracking of an alkane molecule, the hydrocarbon is protonated to form a high-energy transition state that may resemble a firmly coordinated non-classical penta-coordinated carbonium ion [9,10]. Dehydrogenation or cracking of the carbonium ion yield the formation of hydrogen or a paraffin and a carbenium ion that can be desorbed as an alkene or react further [9].

In the general case, a unimolecular decomposition in gaseous phase can be expressed, for example, by the following equation [14]:

$$A(\mathrm{g}) \leftrightarrow B(\mathrm{g}) + C(\mathrm{g})$$

We consider now that the elementary reaction will be the unimolecular surface reaction expressed by the following equation:

$$A_\mathrm{a} \rightarrow B_\mathrm{a} + C_\mathrm{a}, \quad \text{rate constant} : k$$

where A_a, B_a and C_a are the adsorbed species. Consequently, the specific area reaction rate is expressed as follows [14]:

$$r_A = \frac{J}{A} = k\theta_\mathrm{A},$$

where k (mol/m^{2}s), is the rate constant.

It is a very well known experimental fact that the rate constant, k, obeys the Arrhenius law [14–17]:

$$k = A\ \exp\left(-\frac{E_\mathrm{act}}{RT}\right) \tag{1}$$

While the temperature dependence of the equilibrium constant complies with the following relationship:

$$RT\ \ln\ K_\mathrm{A} = -\Delta G_\mathrm{a} = -\Delta H_\mathrm{a} + T\Delta S_\mathrm{a}$$

where ΔG_a, ΔH_a and ΔS_a are the molar integral change of free energy, enthalpy and entropy during adsorption at a given temperature, T [17,18]. That is:

$$K_\mathrm{A} = B\ \exp\left(-\frac{\Delta H_\mathrm{a}}{RT}\right) \tag{2}$$

Consequently, since for low pressures [15–17]:

$$r_\mathrm{A} = kK_\mathrm{A}P_\mathrm{A} = k_\mathrm{obs}P_\mathrm{A}$$

Then, the effective or observed activation energy for the process at low pressures is given by:

$$r_A = kK_\mathrm{A}P_\mathrm{A} = k_\mathrm{obs}P_\mathrm{A} = A\ \exp\left(-\frac{E_\mathrm{obs}}{RT}\right)P_\mathrm{A}$$
$$= C\ \exp\left[-\left(\frac{E_\mathrm{int} + \Delta H_\mathrm{a}}{RT}\right)\right]P_\mathrm{A} \tag{3}$$

In the case of acid high silica zeolites, Haag, have experimentally shown [6] that for monomolecular cracking the apparent or observed activation energy, E_obs, is the sum of the heat of adsorption, ΔH_a, of the alkane and the intrinsic activation energy, E_int:

$$E_\mathrm{obs} = E_\mathrm{int} + \Delta H_\mathrm{a} \tag{4}$$

The fulfillment of Eq. (4), within the experimental error, is manifest from the analysis of the data reported in Table 1 [6]. Therefore, sorption effects are, responsible for the changes in the reaction rates of monomolecular paraffin cracking [6–8].

1.3. Horvath–Kawazoe approach for the description of adsorption in microporous materials for the slit, cylindrical and spherical pore geometry

When a molecule diffuse inside the channels and/or cavities of nanoporous materials, it becomes subjected to: dispersion, repulsion, polarization, field dipole, field gradient quadrupole, adsorbate–adsorbate interactions [17–21], and the acid–base interaction, if the material contains hydroxyl bridge groups [2].

To make a model of an adsorption system, it is necessary to provide a description of the adsorbent–adsorbate and

Table 1
Experimental values for, E_obs, the apparent or observed activation energy, $-\Delta H_\mathrm{obs}$, the sorption enthalpy and the true or intrinsic activation energy, E_int, for the cracking of C_4–C_{10} in H-ZSM-5 [6]

m (carbon number)	E_obs (kJ/mol)	$-\Delta H_\mathrm{obs}$ (kJ/mol)	E_int (kJ/mol)
4	142	63	205
6	125	79	205
8	92	104	196
9	84	113	196
10	67	125	192

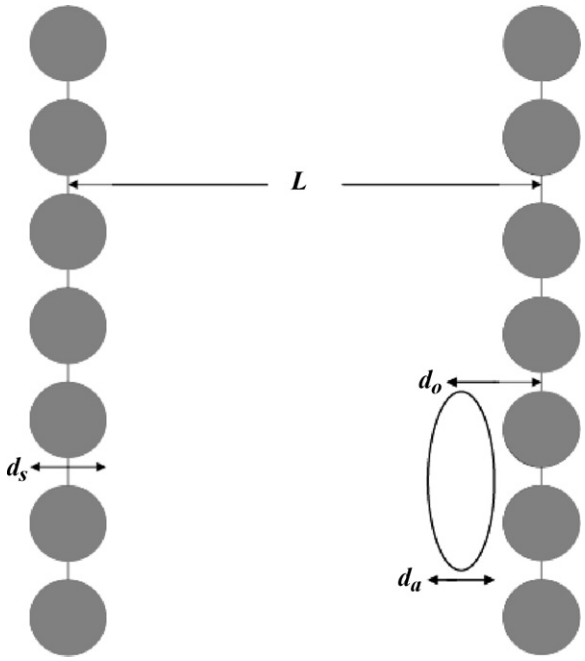

Fig. 1. Parallel slab geometry description of the pore [19].

adsorbate–adsorbate interaction field, and the adsorbent geometry. To describe the interaction field for the situation of our interest here the interactions can be modeled with the help of Lennard-Jones potentials [22–26].

Additionally, the pore geometry have a great influence in the process of adsorption in microporous adsorbents [17,27]; and consequently in the catalytic process [28,29]. In order to consider the effect of the pore geometry on adsorption were worked out various models. In this regard, Horvath and Kawazoe [11] developed a method for calculating the micropore size distribution applying the slit potential model of Everett and Powl [30]. This methodology was later applied by Saito and Foley [12,31] to the case of the cylindrical pore geometry [30] and by Cheng and Yang [13,31] to the case of the spherical pore geometry. All these models has been applied, by numerous authors, not merely to calculate pore size distributions, but as well to get information on other significant properties of the adsorption systems [27].

Now, will be very briefly described the equations and parameters, related with the present paper, of the Horwath–Kawazoe approach for the three pore geometries.

Horvath and Kawazoe [H–K] [11] applied his approach to the case of the interaction of one adsorbate molecule with two infinite lattice planes separated by a distance, L, a potential calculated by Everett and Powl [30] (see Fig. 1):

$$E(z) = \frac{N_{AS}A_{AS}}{2\sigma^4}\left[\left(-\left(\frac{\sigma}{z}\right)^4 + \left(\frac{\sigma}{z}\right)^{10}\right) + \left(-\left(\frac{\sigma}{L-z}\right)^4 + \left(\frac{\sigma}{L-z}\right)^{10}\right)\right] \quad (5)$$

where N_{AS} is the number of solid molecules/surface unit, L the distance between the layers, $\sigma = 0.858d$, where $d = (d_s + d_a)/2$, and, d_s is the diameter of the adsorbent molecule, and, d_a is the diameter of the adsorbate molecule. Besides, z is the internuclear distance between the adsorbate, and adsorbent molecules, and, A_{AS} is the dispersion constant which takes into account the adsorbate–adsorbent interaction. The term A_{AS} is calculated with the help of the Kirkwood–Muller formula [11–13,18,31]:

$$A_{AS} = \frac{6mc^2\alpha_S\alpha_A}{(\alpha_S/\chi_S + \alpha_A/\chi_A)} \quad (6)$$

where m is the mass of an electron, c the speed of light, α_A and, α_S are the polarizabilities of the adsorbate, and the adsorbent molecules, and χ_A and χ_S are the magnetic susceptibilities of the adsorbate and the adsorbent. Later Horwath, and Kawazoe proposed that the potential is increased by the adsorbate–adsorbate interaction, suggesting the following potential [11]

$$\Phi(z) = \frac{N_{AS}A_{AS} + N_{AA}A_{AA}}{2\sigma^4}\left[\left(-\left(\frac{\sigma}{z}\right)^4 + \left(\frac{\sigma}{z}\right)^{10}\right) + \left(-\left(\frac{\sigma}{L-z}\right)^4 + \left(\frac{\sigma}{L-z}\right)^{10}\right)\right] \quad (7)$$

where N_{AA} is the number of adsorbed molecules/surface unit. Besides, A_{AA} calculated with the help of the Kirkwood–Muller formula, is the constant characterizing the adsorbate–adsorbate interactions [11–13,18,31]:

$$A_{AA} = \frac{3mc^2\alpha_A\chi_A}{2} \quad (8)$$

The next step is to obtain the average interaction energy. This is made by averaging the potential expressed by Eq. (8), in this fashion [11]:

$$\xi(L) = N_A\int_d^{L-d}\frac{\Phi(z)dz}{L-2d} \quad (9)$$

where N_A is the Avogadro number to get molar magnitudes. Integrating Eq. (9) is obtained [11]:

$$\xi(L) = N_A\left(\frac{N_{AS}A_{AS} + N_{AA}A_{AA}}{\sigma^4(L-2d)}\right) \times \left(\frac{\sigma^4}{3(L-d)^3} - \frac{\sigma^{10}}{9(L-d)^9} - \frac{\sigma^4}{3d^3} + \frac{\sigma^{10}}{9d^9}\right) \quad (10)$$

In which, $\xi(L)$ is the average potential in a given slit pore obtained by the integration across the effective pore width, and $\Phi(z)$ is the adsorption field inside the slit pore.

For the cylindrical geometry the interaction potential averaged over the cylinder, allow to get an approximate value for the adsorption field in a cylindrical channel [12]. The adsorption process is in this case described with the help of a potential in between a perfect cylindrical pore of infinite length but finite radius, r_p [12]. The calculation was made with the help of a model similar to those developed by Horvath–Kawazoe and a potential calculated by Everett and Powl [30], and it is obtained

for the average interaction energy as follows [12]:

$$\xi(r_p) = \frac{3}{4}\pi N_A \left(\frac{N_{AS}A_{AS} + N_{AA}A_{AA}}{d^4}\right) \times \left(\sum_{k=0}^{\infty}\left[\frac{1}{k+1}\left(1-\frac{d}{r_p}\right)^{2k} \times \left\{\frac{21}{32}\alpha_k\left(\frac{d}{r_p}\right)^{10} - \beta_k\left(\frac{d}{r_p}\right)^{4}\right\}\right]\right) \quad (11)$$

where

$$\varepsilon^* = \frac{3}{10}\left(\frac{N_{AS}A_{AS} + N_{AA}A_{AA}}{d^4}\right) \quad (12)$$

and N_{AS}, d, d_s, d_a, A_{AS}, N_{AA}, and A_{AA}, have the meaning explained in the HK method. Besides [30]:

$$\alpha_k = \left(\frac{\Gamma(-4.5)}{\Gamma(-4.5-k)\Gamma(k+1)}\right)^2$$

and

$$\beta_k = \left(\frac{\Gamma(-1.5)}{\Gamma(-1.5-k)\Gamma(k+1)}\right)^2$$

where $\alpha_0 = \beta_0 = 1$, since $\Gamma(z)$ is the gamma function.

For the spherical pore geometry the average interaction energy between a single adsorbate molecule and the inside wall of the spherical pore cavity of radius, R, was calculated by Cheng and Yang, with the help of a method analogous to those developed by Horvath–Kawazoe, and a potential which has been thoroughly considered in literature [13,31,32]. The calculated average interaction energy is given by [13]:

$$\xi(R) = \frac{6\left(N_1\varepsilon^*_{aA} + N_2\varepsilon^*_{AA}\right)R^3}{(R-d)^3}\left[-\left(\frac{d}{R}\right)^6\left(\frac{1}{12}T_1 + \frac{1}{8}T_2\right) + \left(\frac{d}{R}\right)^{12}\left(\frac{1}{90}T_3 + \frac{1}{80}T_4\right)\right] \quad (13)$$

where

$$N_1 = 4\pi R^2 N_{AS} \quad (14)$$

and

$$N_2 = 4\pi(R-d)^2 N_{AA}; \qquad \varepsilon^*_{aA} = \frac{A_{aA}}{4d^6} \quad \text{and} \quad \varepsilon^*_{AA} = \frac{A_{AA}}{4d^6}$$

Finally

$$T_1 = \frac{1}{(1-(R-d/R))^3} - \frac{1}{(1+(R-d/R))^3};$$

$$T_2 = \frac{1}{(1+(R-d/R))^2} - \frac{1}{(1-(R-d/R))^2};$$

$$T_3 = \frac{1}{(1-(R-d/R))^9} - \frac{1}{(1+(R-d/R))^9} \quad \text{and}$$

$$T_4 = \frac{1}{(1+(R-d/R))^8} - \frac{1}{(1-(R-d/R))^8}$$

2. Calculation of the enthalpy of adsorption of *n*-paraffins in microporous acid catalysts

In the frame of the Horvath and Kawazoe approach it was shown that [11,13,18,31]:

$$\Delta G^{ads} = U_0 + P_a \quad (15)$$

where U_0 and P_0 denotes the adsorbate–adsorbent and adsorbate–adsorbate interaction energies, respectively. The deduction of Eq. (15) is based on the assumption which states that the adsorbed phase behave as an ideal gas in the adsorption space [13,18,31]. One of the authors and collaborators, have demonstrated: that aromatic hydrocarbons, during adsorption in acid zeolites, at about 400 K, behave as a gas in an external force field [33]. Consequently, it is reasonable to suppose that during the cracking process the reacting molecules behave, as well, as an ideal gas in an external field, since cracking takes place at comparatively low pressures and to some extent high temperatures. Then Eq. (15) is applicable.

Now, since the entropy change during adsorption is small [14,20] then:

$$\Delta G^{ads} \approx \Delta H^{ads} \approx U_0 + P_a \quad (16)$$

As was previously commented, for alkanes adsorption the dispersion energy dominates [8,22]. Subsequently, in the case of the adsorption of *n*-alkanes, these hydrocarbons could be approximately described with a united-atom model, where the CH_2 and CH_3 groups are considered as single interaction centers with parameters approximately similar to those characterizing CH_4 [23–26]. Then, the *n*-alkane of, *m* carbons in the frame of this approximation is considered as a linear set of *m* CH_2 groups, if we neglect the effect of one of the, H atoms in the CH_3 terminal groups [23].

In the frame of this model, the alkane–solid interactions are described by a Lennard-Jones potential and the alkane–alkane interactions, between two united atoms is described, as well, by a Lennard-Jones potential [23–26].

Besides, it is necessary to consider that the whole *n*-paraffin interacts with a single acid group, because the, OH groups, in highly siliceous acid zeolites are at a distance of about 10–20 Å depending of the Si/Al relation, distance larger than the length of the hydrocarbon chain [33].

Now, applying the united-atom model for an *n*-alkane, the total average potential for the different geometries of the catalyst pore systems are given by:

$$\xi_T(L) = m\xi^{CH_2}(L) + \xi_{AB}^{C_mH_{2m+2}} \quad (17)$$

$$\xi_T(r_p) = m\xi^{CH_2}(r_p) + \xi_{AB}^{C_mH_{2m+2}} \quad (18)$$

$$\xi_T(R) = m\xi^{CH_2}(R) + \xi_{AB}^{C_mH_{2m+2}} \quad (19)$$

where m is the carbon number, $\xi^{CH_2}(L)$, $\xi^{CH_2}(r_p)$ and $\xi^{CH_2}(R)$, are the average potential for the action of the dispersion and repulsion forces with a, CH_2 group for the three pore geometries, and $\xi_{AB}^{C_mH_{2m+2}}$ is the alkane interaction with the acid site, which do not depends on the pore diameter and the pore geometry.

Table 2
Physical properties of methane and the oxide ion

Atomic species	Polarizability α (10^{-24} cm^3)	Magnetic Susceptibility χ (10^{-29} cm^3)	Diameter d (Å)	Surface density N_s (10^{18} at./m^2)
Methane (CH_4)	2.59 [34]	2.89 [34]	3.0	6.0
Oxide ion	2.50 [34]	1.30 [34]	2.8 [10]	13.1 [10]

Since in the present case the process occurs at relatively low pressures and somewhat high temperatures [4,9]; then we will not consider the adsorbate–adsorbate interaction. Subsequently, the following equations defines: $\xi_{cal}^{CH_2}(L)$, $\xi_{cal}^{CH_2}(r_p)$ and $\xi_{cal}^{CH_2}(R)$:

$$\xi_{cal}^{CH_2}(L) = \left(\frac{N_{AS}A_{AS}}{2\sigma^4(L-2d)}\right) \times \left(\frac{\sigma^4}{3(L-d)^3} - \frac{\sigma^{10}}{9(L-d)^9} - \frac{\sigma^4}{3d^3} + \frac{\sigma^4}{9d^9}\right) \quad (20)$$

$$\xi_{cal}^{CH_2}(r_p) = \frac{3}{4}\pi N_A \left(\frac{N_{AS}A_{AS}}{d^4}\right)\left(\sum_{k=0}^{\infty}\left[\frac{1}{2k+1}\left(1-\frac{d}{r_p}\right)^{2k} \times \left\{\frac{21}{32}\alpha_k\left(\frac{d}{r_p}\right)^{10} - \beta_k\left(\frac{d}{r_p}\right)^4\right\}\right]\right) \quad (21)$$

$$\xi_{cal}^{CH_2}(R) = \frac{6\left(N_1\varepsilon_{aA}^*\right)R^3}{(R-d)^3}\left[-\left(\frac{d}{R}\right)^6\left(\frac{1}{12}T_1 + \frac{1}{8}T_2\right) + \left(\frac{d}{R}\right)^{12}\left(\frac{1}{90}T_3 + \frac{1}{80}T_4\right)\right] \quad (22)$$

In Table 2 are shown a set of values for the parameters, α, χ, d, and, N_s, for CH_4 as adsorbate, and the oxide ion (a zeolite, for example) as adsorbent [13,18,31,34]. Then, with the help of the Kirkwood–Muller formula Eq. (6), it is possible to get the following equations to numerically describe: $\xi_{cal}^{CH_2}(L)$, $\xi_{cal}^{CH_2}(r_p)$ and $\xi_{cal}^{CH_2}(R)$:

$$\xi_{cal}^{CH_2}(L) = \left(\frac{23.21\times10^3}{L-0.60}\right) \times \left(\frac{1.85\times10^{-3}}{(L-0.30)^3} - \frac{2.54\times10^{-7}}{(L-0.30)^9} - 0.050\right) \quad (23)$$

$$\xi_{cal}^{CH_2}(r_p) = 29.65\times10^3\left(\sum_{k=0}^{\infty}\left[\frac{1}{2k+1}\left(1-\frac{d}{r_p}\right)^{2k} \times \left\{\frac{21}{32}\alpha_k\left(\frac{d}{r_p}\right)^{10} - \beta_k\left(\frac{d}{r_p}\right)^4\right\}\right]\right) \quad (24)$$

$$\xi_{cal}^{CH_2}(R) = \frac{4.1R^5}{(R-0.3)^3}\left[-\left(\frac{0.3}{R}\right)^6\left(\frac{1}{12}T_1 + \frac{1}{8}T_2\right) + \left(\frac{0.3}{R}\right)^{12}\left(\frac{1}{90}T_3 + \frac{1}{80}T_4\right)\right] \quad (25)$$

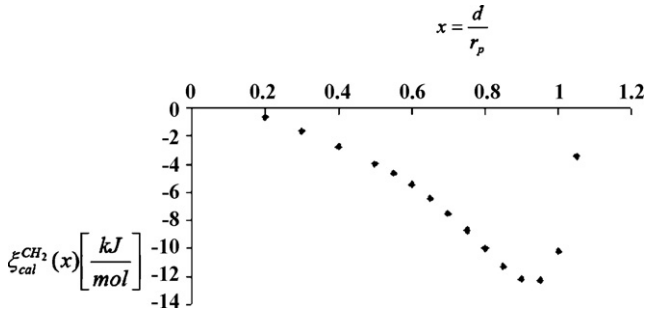

Fig. 2. Graphic representation of Eq. (24).

where L, r_p and R are in nm, and $\xi_{cal}^{CH_2}(\rho)$ where $\rho = L$, r_p, or, R is given in (kJ/mol). In order to give a graphical representation of Eqs. (24) and (25) in Figs. 2 and 3 are plotted these equations. The calculations were carried out with the program system Scientific Notebook [35]. We have no plotted Eq. (23), since the pores of the catalysts discussed in the present paper do not show this pore geometry.

In order calculate the constant in the first term of Eq. (25); Eq. (14) was modified. Because, the FAU framework of zeolite, Y, includes an approximately spherical cavity, with a radius of $R = 6.9$ (Å), [13], known as the supercage, or β cage. Since, this cavity have tetrahedral symmetry, and encompass four 12 MR windows [36]; then, the supercage have four windows each one with a diameter of: $d = 7.4$ (Å) [36]. Then, in order to take into account this fact, the modified area, A_m, was calculated as follows: $A_m = fA$, where $(1-f)$, is the fraction of the surface corresponding to the windows, that is:

$$1 - f = \frac{A_w}{A} = \frac{4\left[\pi(d/2)^2\right]}{4\pi R^2} = \frac{d^2}{4R^2} = 0.29$$

where d is the window diameter and, R is the sphere radius.

Finally, it is evident that, for the different geometries of the pore system:

$$\xi_T(\rho) \approx \Delta H^{ads}$$

where $\rho = L$, r_p, or, R

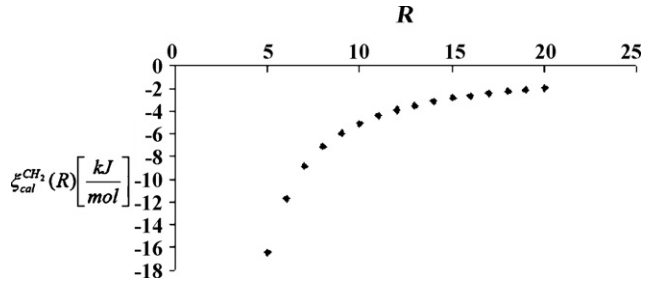

Fig. 3. Graphic representation of Eq. (25).

To conclude the present section it is necessary to make some comments about the merits of the present methodology for the calculation of the adsorption enthalpy of hydrocarbons in nanoporous materials in comparison with former methodologies.

As was above explained, during the cracking process the reacting molecules behave as an ideal gas in an external adsorption field. Consequently, the Horwath–Kawazoe approach is justified, since the average process is possible and Eq. (15) is valid. In this regard, the advantage of the present methodology in comparison to other methods [23–26] is the simplification of the calculations by the help of the average process and Eq. (15), which gives equations which only depend on a set very well defined atomic parameters, which could be found in the literature [11–13,18,31,34] and a unique spatial parameter, that is, the pore size. In addition, the numerical results obtained by the evaluation of these equations adequately agree with experimental results reported in literature.

3. Relation of the activation energy and the calculated enthalpy of adsorption

In the frame of the transition state theory [37,38] the observed activation energy, E_{obs}, for a monomolecular catalytic process in the heterogeneous case is:

$$E_{obs} = E_0 + \Delta H_{ads}[\text{act.complex}],$$

where E_0 is the energy of the reaction without catalyst and, ΔH_{ads}[act.complex] is the adsorption enthalpy of the activated complex [39].

In the monomolecular cracking of *n*-alkanes, catalyzed by an acid zeolite, the activated complex is the adsorbed alkanium ion, i.e. the protonated alkane ($[CR_2H_3^+] - ZO^-$) [8,9]. Therefore:

$$E_{obs} = E_0 + (\Delta H_{ads}[\text{carbocation}]) \quad (26)$$

Subsequently

$$E_{obs} \approx E_0 + m\xi^{CH_2} + \xi_{AB}^{C_mH_{2m+2}} \quad (27)$$

where the concrete expression for, ξ^{CH_2} depends on the pore geometry.

Eq. (27) can be used for the description of the experimental data of adsorption and cracking of *n*-paraffins in H-ZSM-5 zeolite [6] reported in Table 1. If we consider that, $E_0 = E_{int}$, we are able to fit the following equation (see Fig. 4):

$$y = ax + b \quad (28)$$

where $y = E_{obs}$; $x = m$; $a = \xi^{CH_2}(\rho)$, where $\rho = r_p$, and, $b = E_0 + \xi_{AB}^{C_mH_{2m+2}}$. The result of the fitting process was excellent, and the calculated values for the parameters, *a*, and, *b*, were respectively: $a = -12.75$ kJ/mol and $b = 196.5$ kJ/mol.

In Table 3 are reported the calculated values for, $[-(m \cdot a)]$ and its difference with $[-\Delta H_{ads}]$. The reported results indicates that the dispersion term is the most important contribution, as is affirmed in literature [8,22]. Since, if we made an average of the values reported for: $[\Delta H_{ads} - m \cdot a]$ in Table 3, we will get

$$\bar{\xi}_{AB}^{C_mH_{2m+2}} \approx < [\Delta H_{ads} - m \cdot a] > \approx -3 \pm 5\,(\text{kJ/mol})$$

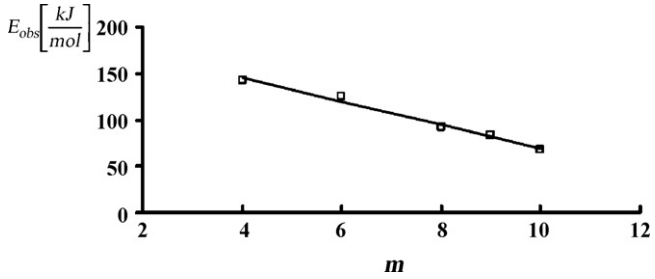

Fig. 4. Fitting of Eq. (27) with the data of the observed activation energy for the cracking of C_4–C_{10} alkanes in H-ZSM-5 versus the number of carbon atoms (m) reported in reference [6].

where $\bar{\xi}_{AB}^{C_mH_{2m+2}}$ is the average acid–base interaction, and $\sigma = \pm 5$ kJ/mol is the standard deviation. Then the calculation of the acid–base interaction term:

$$\xi_{AB}^{C_mH_{2m+2}} \approx \Delta H_{ads} - m(\xi^{CH_2}(\rho)) = \Delta H_{ads} - m \cdot a.$$

Numerically corroborates the statement previously made by other authors affirming that the interaction of the alkane with the acid site is negligible [8,22].

4. Nitrogen adsorption study and pore size analysis of H-ZSM-5, H-mordenite, H-beta, and H-Y zeolites, and the MCM-41 mesoporous molecular sieve

The adsorption study was carried out using N_2 adsorption at 77 K in the following commercial zeolites: H-ZSM-5 (CBV 5020), H-Beta (CP 806) and H-Y (CBV 720) provided by the PQ Corporation, H-mordenite provided by ZEOCAT and a MCM-41 previously synthesized [40,41]. The experiments were carried out with a Quantachrome Autosorb-1 equipment [42].

In Table 4 are reported the structural pore dimensions of the Zeolites: H-ZSM-5, H-MOR, H-Beta, H-USY corresponding to the framework types: MFI, MOR, BEA and FAU [43]. An additional important characteristic of the studied zeolites is the micropore volume, *W*, which is: 0.13 (cm^3/g); for ZSM-5 zeolite, 0.28 (cm^3/g) for Beta zeolite [44,45]; 0.16 (cm^3/g); for the mordenite zeolite and 0.30 (cm^3/g) for zeolite Y [46].

A significant result in the endeavor of obtaining materials showing pore size larger than those of zeolites [3], was the discovery of the M41S family of mesoporous molecular sieves (MMS) [47,48]. These materials possesses exceptionally large uniform pore structures in the mesoscopic scale (2–100 nm) [49,50]. The obtained solid phases are characterized by an ordered, not crystalline, pore wall structure, presenting sharp

Table 3
Figures calculated for $[-(m \cdot a)]$ and its difference with the values reported in Table 1 for $[-\Delta H_{ads}]$

m (carbon number)	$-(m \cdot a)$ (kJ/mol)	$-\Delta H_a$ (kJ/mol)	$(-\Delta H_a - (m \cdot a))$ (kJ/mol)
4	51.0	63	−12.0
6	76.5	79	−2.5
8	102.0	104	−2.0
9	114.75	113	1.75
10	127.5	125	2.5

Table 4
Structural [43] and calculated by adsorption in this work and diffusion methods [33] pore dimensions of the zeolites: H-ZSM-5, H-MOR, H-Beta, H-USY and the mesoporous molecular Sieve: MCM-41

Zeolite	Framework pore diameters (Å)	SF pore diameter (Å)	NLDFT pore diameter (Å)	Max. Kin. diameter (Å)
H-ZSM-5	5.3 × 5.6(10MR) 5.1 × 5.5(10MR) [43]	5.4	–	6 [33]
H-MOR	6.5 × 7.0(12MR) 2.6 × 5.7(8MR) [43]	5.5	–	7
H-Beta	7.6Å × 6.4 Å(12MR) 5.5Å × 5.5 Å(12MR) [43]	5.6	–	7 [33]
H-USY	7.4 (12MR) Cavity: $R = 6.9$ Å [11,43]	6.0	–	8 [46]
MCM-41	39 Å [40,41]	–	36 [40,41]	–

pore size dispersions [51]. In particular the MCM-41 structure have a hexagonal stacking of uniform diameter porous tubes; whose size can be varied from about 15 to more than 100 Å [3,50]. The MMSs have pore volume larger than 0.6 (cm^3/g) [49].

In order to measure the micropore size distribution of the studied zeolites applying the Saito–Foley method [12,31,42], were obtained in the Autosorb-1 the adsorption isotherms of N_2 at 77 K in samples previously degassed at 573 °K during 7 h in high vacuum (10^{-6} Torr).

In Table 4 are reported the pore diameter corresponding to the maximum of the micropore size distribution of the studied samples, specifically: H-ZSM-5, H-mordenite, H-Beta and H-Y zeolites calculated with the help of the SF method [42].

In the case of the MCM-41 mesoporous molecular sieve adsorption study, the previous methodology based in the Saito and Foley method is not applicable. Then, to measure the pore size distribution of the studied MMS was applied the non-local density functional theory (NLDFT)-pore size distribution (PSD) method [18,42,52–54]. To make the NLDFT-PSD determination was obtained in the Autosorb-1 the adsorption isotherms of N_2 at 77 K in a MCM-41 sample previously degassed at 573 °K during 7 h in high vacuum (10^{-6} Torr). In Table 4 is reported the value of the MCM-41 pore diameter corresponding to the maximum of the NLDFT-PSD and the pore diameter determined by XRD [18].

Now, it is necessary to make some additional comments about the pore size of the studied materials. Experimental results related to the diffusion of aromatic hydrocarbons in H-ZSM-5 and H-Beta at temperatures between 300 and 450 K [33,55] indicate that benzene, toluene, and ethylbenzene penetrate freely and rapidly in ZSM-5 and H-Beta, while *m*-xylene and *o*-xylene penetrate only slowly in H-ZSM-5 and fast in H-Beta. Then, it is possible to conclude that the maximum free channel diameter for ZSM-5 is about 6 Å [56,57] and the maximum free diameter for Beta zeolite is around 7 Å (see Table 4) [33], since the minimum kinetic diameters of benzene, toluene, and ethyl benzene are around 5.8 Å and for *o*-xylene and *m*-xylene the values are around 6.8 Å [33,58–60].

It is possible to deduce from the previous discussion that the effective pore size of zeolites is a dynamic parameter which depends on temperature. This is possibly the explanation for the low values obtained with the help of the SF method. The pore sizes estimated with the help of diffusion measurements, at 300–450 K, are higher than those obtained by the SF method. Consequently, since the cracking reaction is carried out at 600–700 K, the pore size that we will apply later to discuss the alkane catalytic cracking are a bit higher than the maximum kinetic diameter reported in Table 4.

Table 5
Experimental values for: E_{obs}, $-\Delta H_{ads}$, and E_{int} for *n*-hexane cracking in H-ZSM-5

Zeolite	E_{obs} (kJ/mol)	$-\Delta H_a$ (kJ/mol)	E_{int} (kJ/mol)
H-ZSM-5	149	86	235
H-MOR	157	69	226
H-USY	177	50	227

H-MOR and H-USY [10].

5. Effect of pore size and geometry in the rate of the unimolecular catalytic cracking reaction

In Tables 5 and 6 are reported the experimental values for: E_{obs}, ΔH_{ads}, and E_{int}. for *n*-hexane cracking in: H-ZSM-5, H-MOR and H-USY zeolites [10], and H-ZSM-5, H-Beta and H-Y zeolites [4]. Now, applying equation:

$$\xi_T(\rho) = m\xi^{CH_2}(\rho) + \xi_{AB}^{C_mH_{2m+2}} \quad (29)$$

It is possible to get

$$\xi_{exp}^{CH_2}(\rho) \approx \frac{\Delta H_a - \xi_{AB}^{C_mH_{2m+2}}}{m} \quad (30)$$

Then, using the data reported in Table 5 [10] and Table 6 [4], and considering that: $\xi_{AB}^{C_mH_{2m+2}} \approx 0$ (kJ/mol) [8,22], in Tables 7 and 8 are reported the experimental values for $\xi_{exp}^{CH_2}$, calculated with Eq. (30) and the theoretical values: $\xi_{cal}^{CH_2}(x)$ and $\xi_{cal}^{CH_2}(R)$ calculated with the help of Eq. (24) and (25) in terms of the variables $x = d/r_p$ and R, using the program system Scientific Notebook [35]. The results obtained with the slit pore model, were not reported since the calculated values do not agree with the experiment. This is an expected outcome, since the zeolite geometry, in general, is possible to be modeled with the cylindrical pore or the spherical pore geometries, but no with the slit pore geometry.

Table 6
Experimental values for: E_{obs}, and E_{int} for *n*-hexane cracking in H-ZSM-5

Zeolite	E_{obs} (kJ/mol)	$-\Delta H_a$ (kJ/mol)	E_{int} (kJ/mol)
H-ZSM-5	108	76	184
H-Beta	93	64	157
H-Y	114	47	161

H-Beta and H-UY [4]. Note: the value for $-\Delta H_{ads}$ was calculate with the help of Eq. (4).

Table 7
Experimental [4,10] and calculated in this work for the cylindrical pore model values of ξ^{CH_2} for H-ZSM-5, H-MOR, H-Beta, H-USY and H-MCM-41

Zeolite	$-\xi^{CH_2}_{exp}$ (kJ/mol)	$-\xi^{CH_2}_{calc}(r_p)$ (kJ/mol)	$d = 2r_p$ (Å)
H-ZSM-5 [10]	14.3	12.5	6.2
H-MOR [10]	11.5	11.0	7.2
H-USY [10]	8.3	8.0	8.4
H-ZSM-5 [4]	12.7	12.5	6.2
H-Beta [4]	10.7	11.0	7.2
H-Y [4]	7.8	8.0	7.2
H-MCM41	–	1.6	20

Table 8
Experimental [4,10] and calculated in this work for the spherical pore model values of ξ^{CH_2} for H-ZSM-5, H-MOR, H-Beta and H-USY

Zeolite	$-\xi^{CH_2}_{exp}$ (kJ/mol)	$-\xi^{CH_2}_{calc}(R)$ (kJ/mol)	R (Å)
H-ZSM-5 [10]	14.3	18700	3.2
H-MOR [10]	11.5	1164	3.6
H-USY [10]	8.3	7.9	7.5
H-ZSM-5 [4]	12.7	18700	3.2
H-Beta [4]	10.7	1164	3.6
H-Y [4]	7.8	7.9	7.5

The results obtained with the cylindrical pore geometry (Table 7) are in a reasonable agreement with the reported experimental data. The values of the pore diameter used in the calculations are a bit higher than the maximum kinetic diameters reported in Table 4, for these zeolites.

For the H-Y zeolite the cylindrical pore model did not provide a completely wrong result; since the pore system of zeolite, *Y*, resembles a three dimensional cylindrical system. However, the appropriate model, for zeolite, *Y*, is the spherical geometry pore [13]; in this regard, the results reported in Table 8 shows that only zeolite, *Y*, is properly described with the spherical geometry pore model.

It is very well known, that the large pores of MCM-41 combined with acidity on the cylindrical walls of these materials were specifically created to perform catalytic cracking of large molecules [3]. With respect to the case of interest here, that is, alkane cracking; Corma and collaborators, have studied the cracking process of *n*-heptane on Al-MCM-41 and USY zeolite, in a microactivity test unit [61]. It has been found in this study that the activity of the USY zeolite is 139 times larger than those of the Al-MCM-41 [3,61].

In Table 7 are reported the values calculated for, $\xi^{CH_2}_{cal}(r_p)$, applying the cylindrical pore model to an hypothetic Al-MCM-41 with a cylindrical pore size of $r_p = 10$ (Å). This result indicate that in these materials the role of adsorption is less than in the case of zeolites. Consequently the cracking rate must be, by far, lower, as was experimentally found by Corma and collaborators [3,61].

6. Conclusions

The Horvath–Kawazoe approach, the Saito–Foley and Cheng–Yang methods, and the united-atom model, were effectively applied for the slit, cylindrical and spherical pore models, in order to get mathematical equations for the numerical description of the enthalpy of adsorption of alkanes in acid nanoporous materials, such as zeolites and mesoporous molecular sieves.

Then, applying concepts created by Haag, Gorte and others, and the transition state theory, the calculated expressions for the enthalpy of adsorption were related with the observed and intrinsic activation energies for the unimolecular catalytic cracking reaction.

The obtained numerical expressions were compared with experimental data, and was shown that it satisfactorily described the literature data related with the monomolecular cracking of *n*-paraffin in acid zeolites. In particular, the results obtained with the cylindrical pore geometry are in good agreement with the reported experimental data. However, for the H-Y zeolite, the spherical model gives a best fitting. In the case of Al-MCM-41 the results of the application of the cylindrical pore model, indicates that in these materials the role of adsorption is less than in the case of zeolites, and then the cracking rate must is by far lower.

Therefore, the obtained results asserts that the catalyst pore structure have an important effect on reactivity in acid nanoporous materials; for that reason, the effect of confinement cannot be described only in terms of an effective pore radius. On the contrary, the pore geometry is significant for the comprehension of how the reaction takes place, as was previously stated by Derouane and collaborators [29].

Besides, it was numerically corroborated that the interaction of the alkane with the acid site is negligible, fact previously reported by Gorte and collaborators [8,22].

Finally, it is necessary to state that the present methodology in comparison with previous methods is mathematically simpler; as a consequence of the averaging procedure and the validity of Eq. (15), which deliver equations, one for each relevant pore geometry, which separately only depends on a group of properly defined atomic parameters, which can be found in the literature, and a single spatial parameter, that is, the pore size. Additionally, the numerical evaluation of these equations gives results which satisfactorily coincide with experimental data reported in literature.

References

[1] J. Biswas, I.E. Maxwell, Appl. Catal. 63 (1990) 197–258.
[2] A. Corma, Chem. Rev. 95 (1995) 559–614.
[3] A. Corma, Chem. Rev. 97 (1997) 2373–2419.
[4] S. Kotrel, M.P. Rosynek, J.H. Lunsford, J. Phys. Chem. B 103 (1999) 818–824.
[5] E.G. Derouane, J. Mol. Catal. A 134 (1998) 29–45.
[6] W.O. Haag, Stud. Surf. Sci. Catal. 84B (1994) 1375–1394.
[7] R.J. Gorte, D. White, Micropor. Mesopor. Mater. 35/36 (2000) 447–455.
[8] L. Yang, K. Trafford, O. Kresnawahjuesa, J. Sepa, R.J. Gorte, D. White, J. Phys. Chem. B 105 (2001) 1935–1942.
[9] H.H. Kung, B.A. Williams, S.M. Babitz, J.T. Miller, R.Q. Snurr, Catal. Today 52 (1999) 91–98.
[10] S.M. Babitz, B.A. Williams, J.T. Miller, R.Q. Snurr, W.O. Haag, H.H. Kung, Appl. Catal. A 179 (1999) 71–86.
[11] G. Horvath, K. Kawazoe, J. Chem. Eng. Jpn. 16 (1983) 470–475.

[12] A. Saito, H.C. Foley, AIChE J. 37 (1991) 429–436.
[13] L.S. Cheng, R.T. Yang, Chem. Eng. Sci. 49 (1994) 2599–2609.
[14] I.N. Levine, Physical Chemistry, 5th ed., McGraw-Hill Higher Education, New York, 2002.
[15] J.M. Thomas, W.J. Thomas, Principle and Practice of Heterogeneous Catalysis, VCH Publishers, New York, 1997.
[16] G.A. Somorjai, Introduction to Surface Chemistry and Catalysis, J. Wiley and Sons, New York, 1994.
[17] R. Roque-Malherbe, Physical Chemistry of Materials, CRC Press, Boca Raton, FL, in press.
[18] R. Roque-Malherbe, Adsorption and Diffusion in Nanoporous Materials, CRC Press, Boca Raton, FL, 2007.
[19] R. Roque-Malherbe, Micropor. Mesopor. Mater. 41 (2000) 227–240.
[20] D.W. Ruthven, Principles of Adsorption and Adsorption Processes, Wiley, New York, 1984.
[21] W. Rudzinski, D.H. Everett, Adsorption of Gases in Heterogeneous Surfaces, Academic Press, London, 1992.
[22] S. Savitz, F. Siperstein, R.J. Gorte, A.L. Myers, J. Phys. Chem. B 102 (1998) 6865–6872.
[23] B. Smit, J. IIja-Siepman, J. Phys. Chem. 98 (1994) 8442–8452.
[24] L. Lu, Q. Wang, Y. Liu, Langmuir 19 (2003) 10617–10623.
[25] L. Lu, Q. Wang, Y. Liu, J. Phys. Chem. B 109 (2005) 8845–8851.
[26] B. Smit, R. Krishna, in: S.M. Auerbach, K.A. Carrado, P.K. Dutta (Eds.), Handbook of Zeolite Science and Technology, Marcell Dekker Inc., New York, 2003, pp. 317–340.
[27] M.L. Pinto, J. Pires, A.P. Carvalho, M.B. de Carvalho, J. Phys. Chem. B 110 (2006) 250–257.
[28] E.G. Derouane, J.M. Andre, a. Lucas, J. Catal. 110 (1988) 58–73.
[29] E.G. Derouane, in: E.G. Derouane, F. Lemos, C. Naccache, F. Ramos-Riveiro (Eds.), Zeolites Microporous Solids: Synthesis, Structure and Reactivity, Kluwer Academic Pub, Dordrecht, 1992, pp. 511–529.
[30] D.H. Everett, J.C. Powl, J. Chem. Soc., Faraday Trans. I. 72 (1976) 619-.
[31] S.U. Rege, R.T. Yang, in: J. Toth (Ed.), Adsorption. Theory, Modeling and Analysis, Marcel Dekker, New York, 2002, pp. 175–207.
[32] P.L. Walker, Chemistry and Physics of Carbon, 2, Dekker, New York, 1966.
[33] R. Roque-Malherbe, R. Wendelbo, A. Mifsud, A. Corma, J. Phys. Chem. 99 (1995) 14064–14071.
[34] D.R. Lide (Ed.), Handbook of Chemistry and Physics, 83rd ed., CRC Press, Boca Raton, FL, 2002–2003.
[35] D.W. Hardy, C.L. Walker, Doing Mathematics with Scientific Workplace and Scientific Notebook, MacKisham Software Inc., Poulsbo, WA, USA, 2003.
[36] R.F. Lobo, in: S.M. Auerbach, K.A. Carrado, P.K. Dutta (Eds.), Handbook of Zeolite Science and Technology, Marcell Dekker Inc., New York, 2003, pp. 65–89.
[37] S. Glasstone, K.J. Laidler, H. Eyring, The Theory of Rate Processes, McGraw-Hill, New York, 1964.
[38] E.M. Sevick, A.T. Bell, D.N. Theodorou, J. Chem. Phys. 98 (1993) 3196–3212.
[39] R.A. van Santen, J. Mol. Catal. A: Chem. 107 (1996) 5–12.
[40] F. Marquez, R. Roque-Malherbe, J. Nanosci. Nanotechnol. 6 (2006) 1114–1118.
[41] R. Roque-Malherbe, F. Marquez, Surf. Interface Anal. 37 (2005) 393–397.
[42] Quantachrome, AUTOSORB-1, Manual, 2003.
[43] Ch. Baerlocher, W.M. Meier, D.H. Olson, Atlas of Zeolite Framework Types, Elsevier, Amsterdam, 2001.
[44] R. Ravinshankar, T. Sen, V. Ramaswami, H.S. Soni, S. Ganapathy, S. Sivansanker, Stud. Surf. Sci. Catal. A 84 (1994) 331–338.
[45] R. Roque Malherbe, R. Wendelbo, Thermochim. Acta 400 (2003) 165–173.
[46] D.W. Breck, Zeolite Molecular Sieves, Wiley, New York, 1974.
[47] C.T. Kresge, M.E. Leonowicz, W.J. Roth, J.C. Vartuli, J.S. Beck, Nature 359 (1992) 710–712.
[48] J.S. Beck, J.C. Vartuli, W.J. Roth, M.E. Leonowicz, C.T. Kresge, K.D. Schmitt, C.T-W. Chu, D.H. Olson, E.W. Sheppard, S.B. McCullen, J.B. Higgins, J.L. Schlenker, J. Am. Chem. Soc. 114 (1992) 10834–10843.
[49] P. Selvam, S.K. Bhatia, C.G. Sonwane, Ind. Eng. Chem. Res. 40 (2001) 3237–3261.
[50] T.J. Barton, L.M. Bull, G. Klemperer, D.A. Loy, B. McEnaney, M. Misono, P.A. Monson, G. Pez, G.W. Scherer, J.C. Vartulli, O.M. Yaghi, Chem. Mater. 11 (1999) 2633–2656.
[51] M.E. Davies, Nature 417 (2002) 813–821.
[52] A.V. Neimark, P.I. Ravikovitch, A. Vishnyakov, J. Phys. Condens. Matter 15 (2003) 347–365.
[53] A.V. Neimark, P.I. Ravikovitch, Micropor. Mesopor. Mater. 44–45 (2001) 697–707.
[54] A.V. Neimark, P.I. Ravikovitch, Colloids Surf. A 187/188 (2001) 11–21.
[55] R. Wendelbo, R. Roque-Malherbe, Micropor. Mater. 10 (1997) 231–246.
[56] J. Karger, D.M. Ruthven, Diffusion in Zeolites and other Microporous Solids, J. Wiley and Sons, New York, 1992.
[57] E.M. Flanigen, J.M. Bennet, R.W. Grose, J.P. Cohen, R.L. Patton, R.M. Kirchner, Nature 271 (1978) 512–516.
[58] A.S.T. Chiang, Ch.-K. Lee, Z.-H. Chang, Zeolites 11 (1991) 380–386.
[59] R.M. Moore, J.R. Katzer, AIChE J. 18 (1972) 816–824.
[60] G. Giannetto, Zeolites, EdIT: Caracas, Venezuela, 1990.
[61] A. Corma, M.S. Grande, V. Gonzalez-Alfaro, A.V. Orchilles, J. Catal. 159 (1996) 375–382.